

Penetration of Projectiles in Composite Laminates

B.P. Patel, S.K. Bhola, M. Ganapathi, and D.P. Makhecha

Institute of Armament Technology, Pune-411 025

ABSTRACT

This paper deals with the prediction of the penetration phenomenon of a cylindro-conical impactor on the kevlar/epoxy-laminated composites using C^0 eight-noded serendipity quadrilateral finite element based on first-order shear deformation theory (FSDT). Local as well as global deformations during impact is considered in the evaluation of indentation, penetration, and perforation phases. Local strains during impact have been evaluated using the hypothesis made from the available experimental observations of bulging during penetration. A detailed parametric study, considering various projectiles and target plate variables, has been carried out to find their effect on the response of the plate, and ballistic parameters, such as ballistic limit and absorbed energy.

Keywords: Composite laminates, penetration phenomenon, FSDT, first-order shear deformation theory, deformation, strain, projectiles, target plates, ballistic limit, advanced composite materials, composite materials, composite armour, shear, delamination

1. INTRODUCTION

The advanced composite materials are being looked upon as the key materials for applications in armour technology during the recent past due to their high stiffness and strength-to-weight ratios. The design of composite armour is a very complex task as compared to conventional single-layer metallic armour, due to the exhibition of coupling among membrane, torsion, and bending strains; weak transverse shear strength, and discontinuity of the mechanical properties along the thickness of the composite laminates. This has drawn attention of several researchers to study the penetration phenomenon in composite armours.

Various theories proposed for predicting the characteristics of penetration of composite laminates by different projectiles have been reviewed by Abrate¹, Cantwell and Morton². The work on penetration

under low velocity impact is extensively dealt in the literature³⁻⁷. The impact resistance and subsequent load-bearing capacity of composites depends on many factors, such as fibre and matrix properties, lay-up, number of layers^{4,5}, etc.

The impact, resulting in complete penetration of laminates caused due to the high velocity, is called ballistic impact and is of major concern to the armour designers. Further, the damage caused to the armour under high velocity impact is quite significant and has major effects on the dynamic properties of the laminates. Modelling of penetration and perforation in brittle materials like glass fibre reinforcing a thermoset matrix has been done by Cantwell and Morton⁸; Goldsmith⁹, *et al.* and is primarily based on shear caused during penetration, which acts along the lateral surface of the projectile.

Ductile composite materials, such as laminates reinforced by aramid or polyethylene fibres, have been studied by Navarro¹⁰ and Zhu^{11,12}, *et al.* Analytical models based on dynamic behaviour of fibres have been proposed¹⁰. Zhu¹², *et al.*, based on the experimental observations¹¹, have proposed an analytical model to predict the perforation and the ballistic limit for kevlar/epoxy-laminated composites impacted by conical projectiles, considering local and global deformations.

Some work on ceramic-faced hybrid composites have been carried out by Chocron and Sanchez¹³, and Fellows and Barton¹⁴ based on analytical solutions. Cantwell and Morton⁸ have predicted the ballistic limit for carbon fibre-reinforced plastics (CFRPs) by accounting the energy dissipation in delamination, deformation, and shear. These models can predict the energy absorption for thin laminates with reasonable success but underestimate the same for thick laminates, due to the absence of a well-defined conical damaged zone.

Lee and Sun¹⁵ have used quasi-static finite element analysis to simulate the penetration process in graphite/epoxy-laminated composites, wherein the penetration criterion is based on static punch tests. Wen¹⁶, *et al.* have proposed an empirical formula for predicting the ballistic limit based on experimental observations, whereas Wen¹⁷ has predicted penetration and perforation of the fibre-reinforced plastic (FRP) laminates based on mean pressure offered by the laminated targets to resist the penetrator. The resistive pressure offered is divided into quasi-static resistive pressure applied perpendicular to the surface due to elastic-plastic deformation of the FRP and the dynamic resistive pressure arising from velocity effects.

The models described above are primarily based on conservation of energy and no progressive damage propagation is considered except by Zhu¹², *et al.* To study the influence of various parameters affecting the penetration process, the model should be able to describe the physical events, such as indentation, fibre breakage, delamination, bulging occurring during penetration. In view of this, a C⁰ eight-noded quadrilateral serendipity plate finite element with five DOFs per node has been used to study the

response of target plate due to impact of conical projectiles. Both local as well as global responses of laminates, depending on the impact velocity, affect the penetration process. The discrete equations of motion are integrated numerically, using Newmark's direct integration technique.

The three phases of ballistic impact (indentation, perforation, and exit) observed during experimentation are incorporated in this model. These three phases have been modelled with distinct start and termination phenomenon. The termination of the indentation occurs when the first fibre breakage at the distal side takes place. The breakage of fibres has been modelled based on the critical fibre breakage strain of 4 per cent for kevlar fibres. The strain in fibres can be due to global as well as local deformation, which is either due to bulging or physical deformation of fibre around the indenter. The model is based on the assumptions, such as rigidity of projectile, spherical bulging on the distal side of the target. Local fibre deformation occurs around the bulge or the indenter cone. The friction effect gradually dominates as the projectile exits the laminate. The resistance offered by the damaged plate is incorporated in the form of a factor, which is proportional to the number of fibres broken. Matrix cracking is neglected as it is negligible in case of kevlar epoxy-laminated composites¹¹.

2. FORMULATION

A composite plate with arbitrary lamination is considered with coordinates x, y along the in-plane directions, and z along the thickness direction, with its origin at the mid-plane. The displacements at any point (x, y, z) from the median surface are expressed as function of mid-plane displacement u_0, v_0, w_0 and independent rotation θ_x, θ_y as

$$\begin{aligned} u(x, y, z, t) &= u_0(x, y, t) + z \theta_x(x, y, t) \\ v(x, y, z, t) &= v_0(x, y, t) + z \theta_y(x, y, t) \\ w(x, y, z, t) &= w_0(x, y, t) \end{aligned} \quad (1)$$

Using the above displacement field, the strains in the laminate can be expressed as

$$\{\epsilon\} = \begin{Bmatrix} \epsilon_{xx} \\ \epsilon_{yy} \\ \gamma_{xy} \end{Bmatrix} = \{\epsilon_0\} + z\{\epsilon_1\}$$

$$\{\epsilon_s\} = \begin{Bmatrix} \gamma_{xz} \\ \gamma_{yz} \end{Bmatrix} \quad (2)$$

where

$$\{\epsilon_0\} = \begin{Bmatrix} u_{0,x} \\ v_{0,y} \\ u_{0,y} + v_{0,x} \end{Bmatrix}; \quad \{\epsilon_1\} = \begin{Bmatrix} \theta_{x,x} \\ \theta_{y,y} \\ \theta_{x,y} + \theta_{y,x} \end{Bmatrix}$$

$$\{\epsilon_s\} = \begin{Bmatrix} \theta_x + w_{0,x} \\ \theta_y + w_{0,y} \end{Bmatrix} \quad (3)$$

The stress and moment resultants can be written in a matrix form as

$$\begin{Bmatrix} N \\ M \end{Bmatrix} = \begin{bmatrix} A & B \\ B & D \end{bmatrix} \begin{Bmatrix} \epsilon_0 \\ \epsilon_1 \end{Bmatrix}$$

where

$$A = \int [\bar{Q}] dz, \quad B = \int z [\bar{Q}] dz$$

$$D = \int z^2 [\bar{Q}] dz \quad (4)$$

Similarly, the transverse shear stress resultant $\{Q\}$ representing the quantities (Q_{xz}, Q_{yz}) are related to the transverse shear strains $\{\epsilon_s\}$ through the constitutive relations as

$$\{Q\} = [E] \{\epsilon_s\}$$

where

$$[E] = \int [\bar{Q}] dz \quad (5)$$

Here, the terms of $[\bar{Q}]$ matrix are referred to the laminate axes and can be obtained from the $[\bar{Q}]$ corresponding to the fibre directions with the appropriate transformation¹⁸.

The governing equations are obtained by applying Lagrangian equations of motion given by

$$\frac{d}{dt} [\partial(T-U)/\partial \dot{\delta}_i] - [\partial(T-U)/\partial \delta_i] = F_i;$$

$$i = 1 \text{ to } n \quad (6)$$

where U is the strain energy contributions due to the in-plane and transverse stresses. $\{\delta\} = \{\delta_1, \delta_2, \dots, \delta_n\}^T$ is the vector of the DOFs/generalised coordinates and F_i is the generalised force. A dot over the variables represents the partial derivative wrt time.

The strain energy (U) can be written as

$$U(\delta) = \frac{1}{2} \{\delta\}^T [K] \{\delta\} \quad (7)$$

where $[K]$ is the stiffness matrix.

The kinetic energy of the plate is given by

$$T(\delta) = \frac{1}{2} \iint \left[\sum_{k=1}^n \int_{h_k}^{h_{k+1}} \rho_k \{\dot{u} \ \dot{v} \ \dot{w}\} \{\dot{u} \ \dot{v} \ \dot{w}\}^T dz \right] dx dy \quad (8)$$

where ρ_k is the mass density of the k^{th} layer and h_k, h_{k+1} are the coordinates of laminates corresponding to the bottom and top surfaces of the k^{th} layer.

Substituting Eqns (7) and (8) in Eqn (6), one obtains the governing equation for the plate as

$$[M] \{\ddot{\delta}\} + [K] \{\delta\} = \{F\} \quad (9)$$

where $[M]$ is the mass matrix and $\{F\}$ is the force vector due to impact.

Governing equation for the projectile can be written as

$$m_p \ddot{w}_p = F_p \quad (10)$$

where m_p and w_p are the mass and the displacement of the projectile, and F_p is the force acting on the projectile due to the resistance offered by the laminate.

The Eqns (9) and (10) are solved simultaneously using Newmark's direct integration technique.

2.1 Strain due to Local Deformation

Local deformation is modelled based on the spherical bulging observed in the experimental work¹¹. It is assumed that the volume of bulge formed is the same as the volume displaced by the indenter into the laminate. Based on these assumptions, the half-cone angle (ξ) of the bulge, as shown in the Fig. 1, can be determined from equation given by

$$\left(\frac{w_r}{h} \sin \xi\right)^3 \tan^2 \beta - \left(\frac{w_r}{h} \tan \beta + \tan \xi\right)^3 \times (1 - \cos \xi)^2 (2 + \cos \xi) = 0 \tag{11}$$

and the radius of the spherical bulge (r) is given by

$$r = \frac{w_r \tan \beta + h \tan \xi}{\sin \xi} \tag{12}$$

where w_r is the penetration of the projectile, h is the total thickness of the laminate, and β is the semi-cone angle of the tip of the cylindro-conical projectile.

The local strain (ϵ_l) in fibres that undergo bulging is determined based on the geodesic on the surface of the sphere in a portion of a great circle and is given by¹²

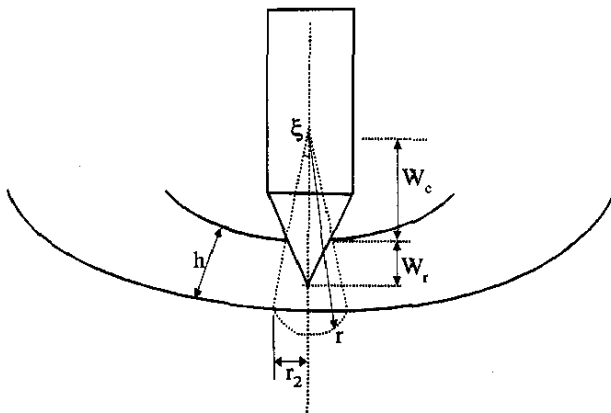


Figure 1. Global deflection and bulging

$$\epsilon_l = \frac{\sin^{-1} \left[\frac{y_0}{\sqrt{x_0^2 + y_0^2}} \sin \xi \right]}{\frac{y_0}{\sqrt{x_0^2 + y_0^2}} \sin \xi} - 1 \tag{13}$$

where x_0 and y_0 are the coordinates of the fibre point at the intersection of spherical bulge surface with laminate as shown in the Fig. 2.

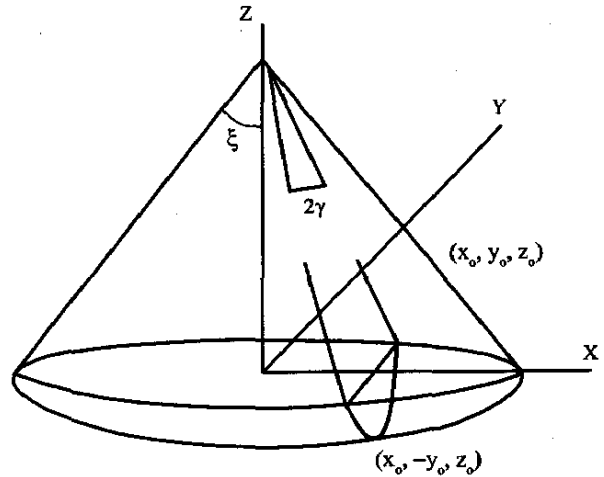


Figure 2. Geodesic due to fibre deformation around the surface of sphere.

The local strain ϵ_l for the fibres that are in contact with the indenter, due to the stretching around the indenter surface, is given by¹²

$$\epsilon_l = \frac{\frac{z_0}{\cos \beta} \sin \left[\sin \beta \sin^{-1} \left(\frac{y_0}{z_0 \tan \beta} \right) \right] - y_0}{y_0} \tag{14}$$

where y_0 and z_0 are the coordinates of the point where contact of fibre with indenter surface terminates as shown in the Fig. 3.

2.2 Resistive Strength of Laminate

The resistive force of the laminate for the indentation phase is given by

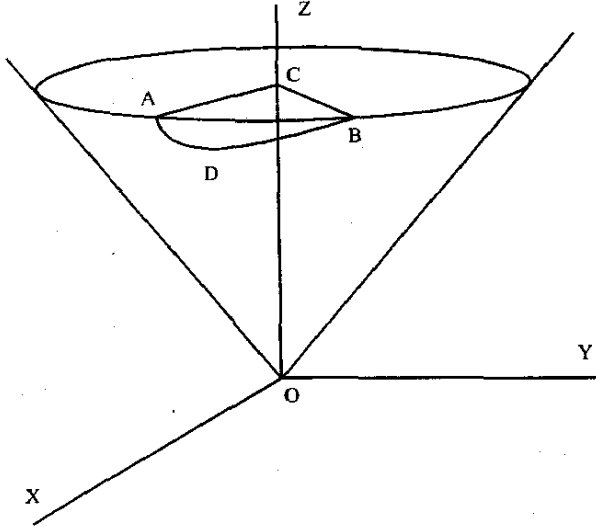


Figure 3. Geodesic due to fibre deformation around the cone surface.

$$F_p = p_m A_p = p_m \pi w_r^2 \tan^2 \beta \quad (15)$$

where p_m is the mean pressure proportional to the yield stress of the material along the direction of impact and A_p is the projected contact area. The termination of indentation phase is assumed when any fibre in the distal side breaks.

The resistance of laminate during penetration phase is governed by the ratio of broken and unbroken fibres in the contact zone and it can be expressed as

$$F = p_m A_p (1 - d_m) = p_m (1 - d_m) \pi w_r^2 \tan^2 \beta \quad (16)$$

where d_m is the damage parameter and is defined by

$$d_m = \frac{N_d}{N_u + N_d}$$

where N_d and N_u are the number of damaged and undamaged fibres in front of the contact zone.

During the exit stage of the projectile, the only resistive force offered by the laminate is the frictional force (F_m) between the laminates and the shank portion of the projectile. This stage terminates

when the projectile shank has completely separated from the target or when the projectile velocity becomes zero.

3. RESULTS & DISCUSSION

The above formulation is used to study the penetration of cylindro-conical rigid projectiles on the clamped laminated square plates with in-plane 100 mm × 100 mm. Based on progressive mesh refinement, a 16 × 16 non-uniform mesh is found to be adequate for the prediction of the global strain due to impact. The ratio of the sizes of the elements near the point of impact and away from the contact zone is kept as 2/5.

The material properties for kevlar/epoxy, as obtained from the literature, and used here are:

$$E_L = 76 \text{ GPa}, E_T = 5.6 \text{ GPa}$$

$$G_{LT} = G_{TT} = 2.8 \text{ GPa}, \nu_{LT} = \nu_{TT} = 0.25$$

$$\rho = 1230 \text{ kg/m}^3$$

$$p_m = 261 \text{ MPa}, F_\mu = 1068 \text{ N.}$$

where E , G and ν are the Young's modulus, shear modulus, and Poisson's ratio. Subscripts L and T are the longitudinal and the transverse directions, respectively, wrt the fibres. The first layer corresponds to bottommost layer and the layer-angle is measured from x -axis in an anticlockwise direction and all the layers are of equal thickness. It may be noted here that the laminate properties are considered for the analysis in the work of Zhu¹¹, *et al.*, whereas the above mentioned material properties are introduced in the present analysis.

The projectile parameters assumed are:

$$\text{Mass} = 28.9 \text{ g}$$

$$\text{Diameter} = 12.7 \text{ mm}$$

$$\text{Length} = 38.1 \text{ mm}$$

$$\text{Tip-cone angle } (\beta) = 60^\circ$$

The interfibre distance is taken as 6 μm . The clamped-clamped boundary conditions considered here are:

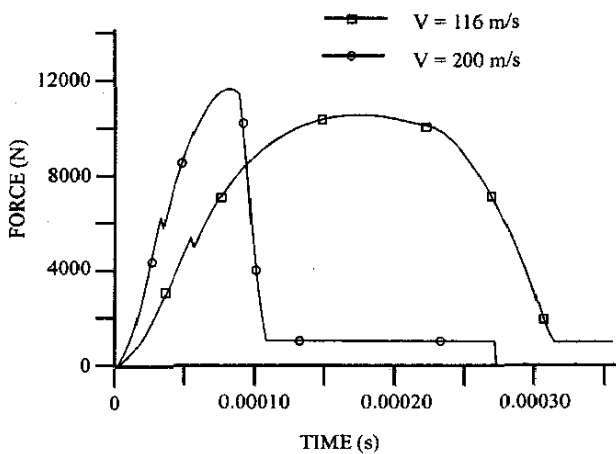


Figure 4(a). Impact force history of 10-layered cross-ply laminated plate.

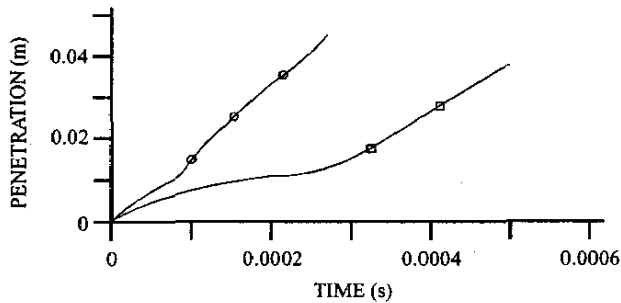


Figure 4(b). Penetration history of projectile on 10-layered laminated plate.

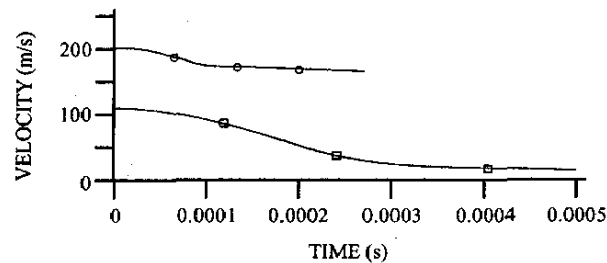


Figure 4(c). Projectile velocity history for different initial velocities.

$$u_0 = v_0 = w_0 = \theta_x = \theta_y = 0$$

$$\text{at } x = 0, a \text{ and } y = 0, b.$$

Here, a and b are the length and the width of the plate.

Firstly, for the purpose of validation, the ten-layered cross-ply laminated plate of 6.35 mm total

thickness¹¹ is analysed. The ballistic limit computed from the present investigation is found to be 106.95 m/s, which is in very good agreement with the experimental value of 109 m/s given by Zhu¹¹, *et al.* Further, the force, penetration, and residual velocity versus time curves are shown in the Fig. 4.

In the force history, sudden drop off in the force magnitude corresponds to the termination of indentation phase and the start of penetration phase. After this point, again, the contact force increases due to the increase in the contact area, and it reaches to a peak value. Further, decrease in force magnitude is due to the fibre breakage. In the last phase of exit, the constant force is due to only frictional force between the perforated hole in the laminate and the projectile shank. The results are qualitatively similar to the experimental results given by Zhu¹¹, *et al.* Thus, the model represents the penetration phenomenon reasonably well.

Next, the parametric study is carried out considering the various parameters, such as target thickness, lay-up, tip angle of projectile, and the initial velocity of the projectile. To analyse the target thickness effect, 10-, 15- and 20-layered cross-ply laminated plates with total thicknesses of 6.35 mm, 9.525 mm, and 12.7 mm, respectively are considered. The initial kinetic energy of the projectile is kept constant at 578 J in all the three cases. Ballistic limit versus thickness graph obtained by the present formulation is shown in the Fig 5.

It can be seen from this figure that the ballistic limit is linearly proportional to the thickness. The results obtained are slightly low compared to those

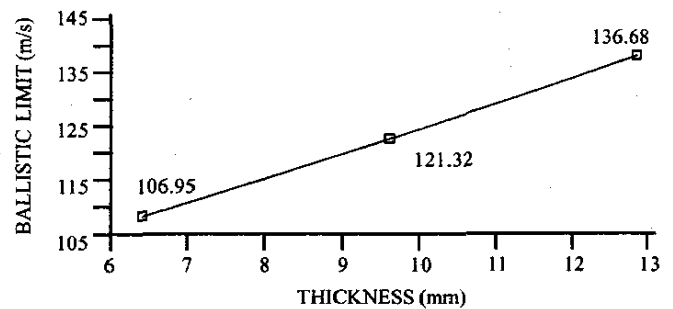


Figure 5. Effect of thickness on ballistic limit

given by Zhu¹¹, *et al.* This is attributed to the difference in the material/lamination properties used in the present study and given by Zhu¹¹, *et al.* In Fig. 6, absorbed energy versus time graph is depicted and it shows that the rate of energy absorption increases with thickness during the initial phase of penetration.

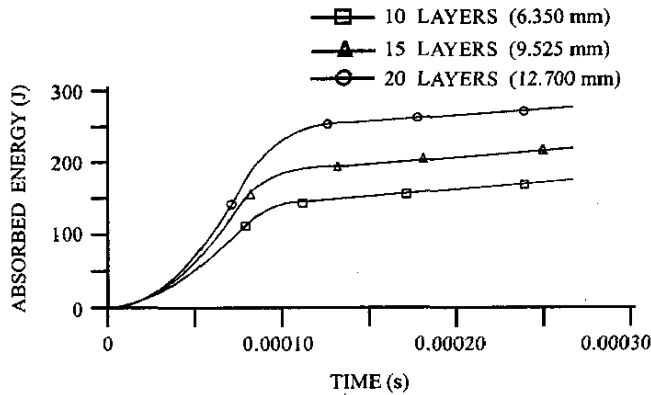


Figure 6. Variation of absorbed energy for different thicknesses of target plate.

The influence of tip angle of penetrator is investigated by considering 60° and 120° projectiles impacting on 6.35 mm thick 10-layered laminate. The force and velocity histories are shown in the Figs 7(a) and 7(b). The ballistic limits obtained for 60° and 120° tip angles of penetrators are found to be 104.99 m/s and 141.42 m/s. Hence, it can be stated that the laminated composite plate is able to resist the blunt projectile efficiently. It is also observed that the peak force on impact and time of exit of 120° projectile is more than that of 60° projectile. The time of exit of the projectiles is found to be 267 μs and 233 μs for 120° and 60°, respectively, thus the duration of exit phase is more for 120° penetrator.

Parametric study for the effect of initial velocity is carried out by keeping the initial kinetic energy constant at 578 J. Figure 8(a) shows that the ballistic limit increases with the initial velocity for same initial kinetic energy and it follows a linear relationship with initial velocity of impact. It can be noticed from Fig. 8(b) that at low initial velocities near the ballistic limit, the plate vibrates with higher amplitude and for longer time period and the response of the plate changes with increase in impact velocity,

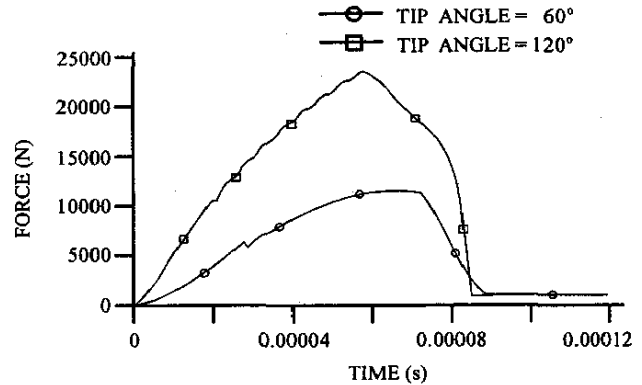


Figure 7(a). Effect of tip angle on force history

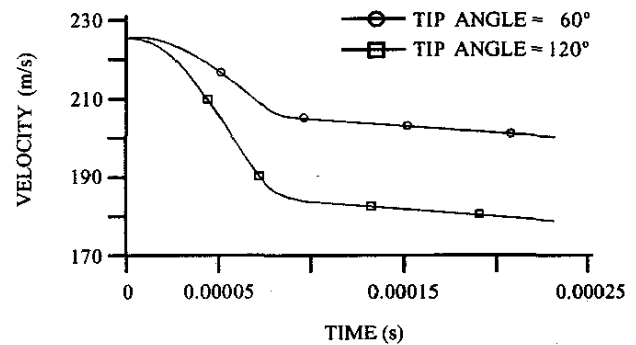


Figure 7(b). Variation of projectile velocity with time for different tip angles of penetrator.

ie, response shows secondary peaks and decrease in response time period.

It is hoped that the present study will be useful for the armour designers in providing an insight into the ballistic impact of projectiles on laminated structures.

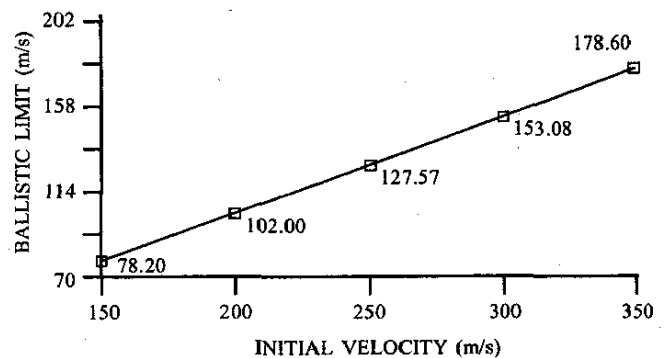


Figure 8(a). Variation of ballistic limit with initial velocities.

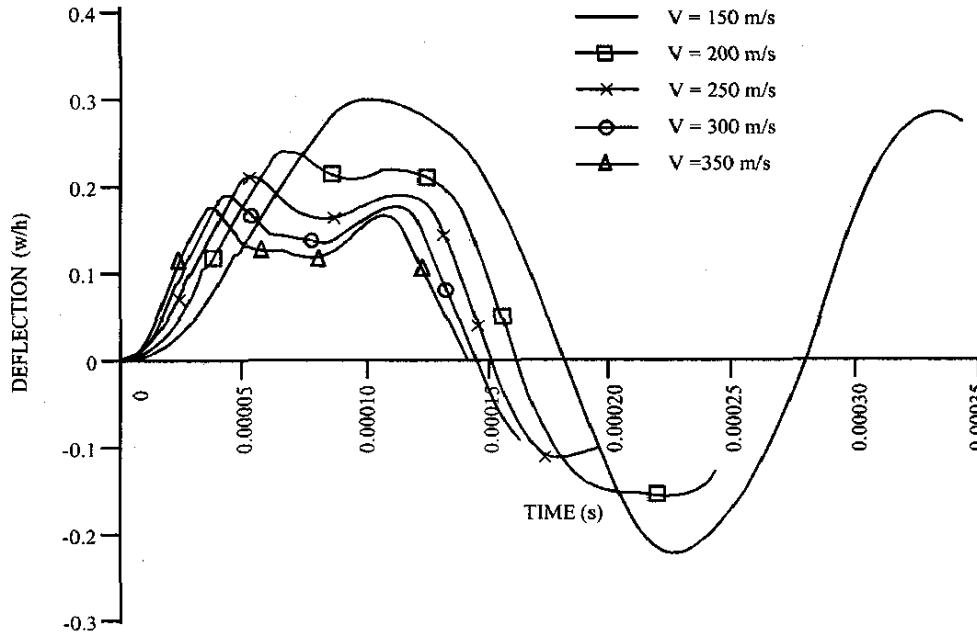


Figure 8(b). Plate deflection history for different initial velocities

4. CONCLUSIONS

Experimental studies of ballistic impact on laminated composites is pursued aggressively in the literature and valuable insights have been gained on ballistic impact on composites. The present finite element model includes three phases of ballistic impact and it represents the penetration phenomenon reasonably well. The variation of peak force, energy absorption, and ballistic limit due to impact, for various input parameters, are similar to the experimental observations made by various researchers. Some of the conclusions made from the present study are:

- (a) Ballistic impact is characterised by the three phases, namely indentation, perforation, and exit.
- (b) Ballistic limit is linearly related to the thickness of the laminated composites.
- (c) The absorbed energy and the peak force increase with thickness for a given impact energy.
- (d) For the same impact energy, the perforation energy is independent of impact velocity, and the ballistic limit increases with the initial velocity.

The exit velocity increases linearly with the impact velocity.

- (e) The effect of initial kinetic energy is reflected by increase in the peak force with increase in impact velocity. For impact velocity much above the ballistic limit, the exit velocity increases linearly with impact velocity but drops suddenly as the impact velocity approaches the ballistic limit. As the impact velocity reaches the ballistic limit, the target plate shows excessive vibrations during perforation process.
- (f) The ballistic limit and the peak resistive force of the plate are more for blunt impacters. First fibre breakage occurs earlier in case of blunt projectiles compared to sharp projectiles.

REFERENCES

1. Abrate, S. Impact on laminated composites: Recent advances. *Appl. Mech. Rev.*, 1994, **47**, 517-44.
2. Cantwell, W.J. & Morton, J. The impact resistance of composite materials: A review. *Composites*, 1991, **22**, 347-62.

3. Tracy, J.J.; Dimas, D.J. & Pardoen, G.C. The effect of impact damage on the dynamic properties of laminated composite plates. *In Proceedings of the 5th International Conference on Composite Materials, ICCM-V, 1985.* pp. 111-25.
4. Cantwell, W.J. & Morton, J. Comparison of low velocity and high velocity impact response of CFRP. *Composites*, 1989, **20**, 545-51.
5. Prewo, K.M. The importance of fibres in achieving impact-tolerant composites. *Phil. Trans. R. Soc. London*, 1980, **A 294**, 551-58.
6. Palazotto, A.N.; Herup, E.J. & Gummadi, L.N.B. Finite element analysis of low velocity impact on composite sandwich plates. *Composite Structures*, 2000, **49**, 209-27.
7. Palazotto, A.N.; Herup, E.J. & Gummadi, L.N.B. Finite element analysis of low velocity impact on composite sandwich plates. *In Proceedings of the 1999 AIAA/ASME/ASCE/AHS/ASC structures, Structural Dynamics and Materials Conference and Exhibit, Vol. 1, 1999.* pp. 739-49.
8. Cantwell, W.J. & Morton, J. Impact perforation of carbon fiber-reinforced plastic. *Comp. Sci. Tech.*, 1990, **38**, 119-41.
9. Goldsmith, W. Dharan, C.K.H. & Chang, H. Quasi-static and ballistic perforation of carbon fibre laminates. *Int. J. Solids Struct.*, 1995, **32**, 89-103.
10. Navarro, C. Simplified modelling of the ballistic behaviour of fabrics and fiber-reinforced polymeric matrix composites. *Key Eng. Mat.*, 1998, **141-143**, 383-403.
11. Zhu, G; Goldsmith, W. & Dharan, C.K.H. Penetration of laminated kevlar by projectiles-I Experimental investigation. *Int. J. Solids Struct.*, 1992, **29**, 399-420.
12. Zhu, G; Goldsmith, W. & Dharan, C.K.H. Penetration of laminated kevlar by projectiles-II Analytical model. *Int. J. Solids Struct.*, 1992, **29**, 421-36.
13. Chocron Benloulo, I.S & Sanchez Galvez, V. A new analytical model to simulate impact onto ceramic/composite armours. *Int. J. Impact*, 1998, **21**, 461-71.
14. Fellows, N.A. & Barton, P.C. Development of impact model for ceramic-faced semi-infinite armour. *Int. J. Impact*, 1999, **22**, 793-811.
15. Lee, S.W.R. & Sun, C.T. Dynamic penetration of graphite epoxy laminates impacted by a blunt-ended projectile. *Comp. Sci. Tech.*, 1993, **49**, 369-80.
16. Wen, H.M; Reddy, T.Y.; Reid S.R. & Soden, P.D. Indentation, penetration, and perforation of composite laminates and sandwich panels under quasi-static and projectile loading. *Key Eng. Mat.*, 1998, **141-143**, 501-52.
17. Wen, H.M. Predicting the penetration and perforation of FRP laminates struck normally by projectiles with different nose shapes. *Composite Structures*, 2000, **49**, 321-29.
18. Jones, R. M. *Mechanics of composite materials.* McGraw Hill, New York, 1975.